JACS
JOURNAL OF THE AMERICAN CHEMICAL SOCIETY
Article
pubs.acs.org/JACS

Stepwise Photocatalytic Dissociation of Methanol and Water on TiO_2(110)

Qing Guo,[†] Chenbiao Xu,[†,§] Zefeng Ren,[†] Wenshao Yang,[†] Zhibo Ma,[†] Dongxu Dai,[†] Hongjun Fan,*[,†] Timothy K. Minton,[‡,∥,*] and Xueming Yang*[,†]

[†]State Key Laboratory of Molecular Reaction Dynamics, Dalian Institute of Chemical Physics, 457 Zhongshan Road, Dalian 116023, Liaoning, P. R. China

[‡]Department of Chemistry and Biochemistry, Montana State University, Bozeman, Montana 59717, United States

Supporting Information

ABSTRACT: We have investigated the photocatalysis of partially deuterated methanol (CD_3OH) and H_2O on TiO_2(110) at 400 nm using a newly developed photocatalysis apparatus in combination with theoretical calculations. Photocatalyzed products, CD_2O on Ti_{5c} sites, and H and D atoms on bridge-bonded oxygen (BBO) sites from CD_3OH have been clearly detected, while no evidence of H_2O photocatalysis was found. The experimental results show that dissociation of CD_3OH on TiO_2(110) occurs in a stepwise manner in which the O−H dissociation proceeds first and is then followed by C−D dissociation. Theoretical calculations indicate that the high reverse barrier to C−D recombination and the facile desorption of CD_2O make photocatalytic methanol dissociation on TiO_2(110) proceed efficiently. Theoretical results also reveal that the reverse reactions, i.e, O−H recombination after H_2O photocatalytic dissociation on TiO_2(110), may occur easily, thus inhibiting efficient photocatalytic water splitting.

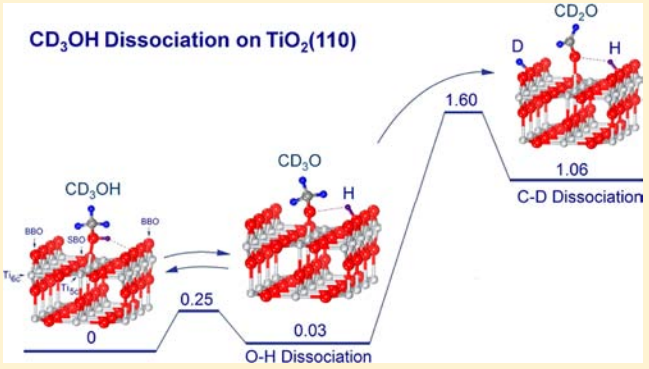

INTRODUCTION

Titanium dioxide has been extensively investigated as a catalyst or photocatalyst,[1−11] particularly in applications involving photodegradation of organic molecules and water splitting,[5,12,13] which have important implications in environmental remediation and clean energy. Pure TiO_2 is apparently not photocatalytically active for splitting water to produce hydrogen,[14] but the addition of methanol to water can dramatically enhance the photocatalytic activity for hydrogen production.[15] Therefore, understanding the key differences between the photocatalytic chemistry of methanol and water on a model TiO_2 surface at the molecular level may provide valuable insight into the dynamics of photocatalysis that would enhance efforts for developing new and efficient photocatalysts for water splitting.

Theoretical and experimental studies often focus on TiO_2(110) as a model surface,[6,16] with the methanol/TiO_2(110) system serving as a model for photocatalysis on TiO_2.[17−20] Henderson and co-workers[18] conducted a temperature-programmed desorption (TPD) study of CH_3OH on TiO_2(110) and concluded that the majority of the CH_3OH molecules are adsorbed in molecular form. This conclusion is consistent with a scanning tunneling microscopy study by Dohnalek et al.[10] that showed that methanol molecules are adsorbed molecularly on the Ti_{5c} sites and are dissociated only at bridge-bonded oxygen (BBO) vacancy sites. The photocatalysis of CH_3OH on TiO_2(110) was investigated in a two-photon photoemission (2PPE) experiment, which inferred the presence of an excited electronic state on the surface.[20,21] Zhou et al. attributed this surface state to a photocatalytic dissociated state of methanol using a time-dependent 2PPE (TD-2PPE) technique.[22] They also used a combination of photoexcitation with STM and found that 400 nm light could induce dissociation of methanol on the surface, and they assigned the dissociated state as methoxy (CH_3O) on a Ti_{5c} site and a hydrogen atom on a BBO site. Shen and Henderson subsequently conducted a TPD study of CH_3OH photocatalysis on TiO_2(110), and they detected a formaldehyde (H_2CO) product and suggested that CH_3O is the active intermediate that leads to H_2CO.[23] While the mechanism of methanol photocatalysis on TiO_2(110) is slowly being revealed, the results to date do not unambiguously reveal the reactions that lead from CH_3OH to H_2CO. By understanding this reaction sequence in detail and comparing it to analogous photocatalytic reactions of H_2O on TiO_2(110), we hope to learn the important features of the processes that give rise to the difference in the photocatalytic activity of CH_3OH and H_2O on TiO_2(110).

Received: April 27, 2012
Published: July 13, 2012

   dx.doi.org/10.1021/ja304049x | J. Am. Chem. Soc. 2012, 134, 13366−13373

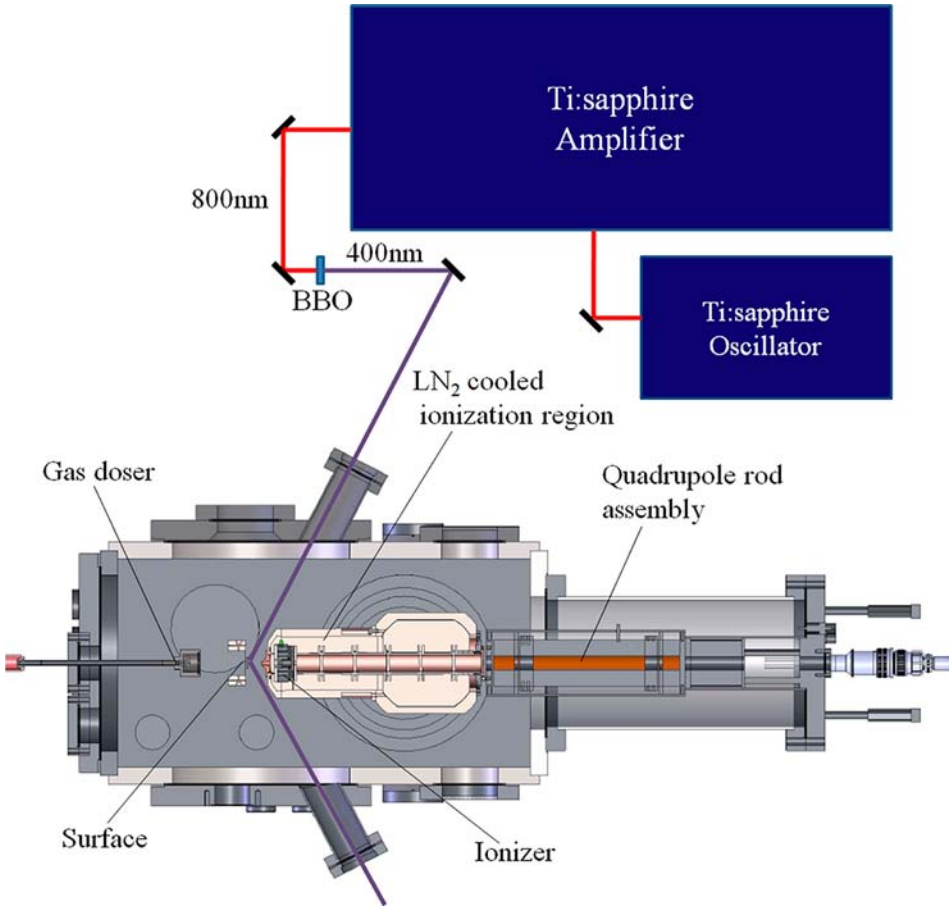

Figure 1. Schematic diagram of the surface photocatalysis apparatus.

We have conducted a combined experiment/theory study using laser-induced photocatalysis and temperature-programmed desorption (TPD) mass spectrometry to probe nascent products from the photocatalytic dissociation of methanol on the TiO_2 surface and density functional theory to calculate stationary-point structures and energies along the reaction path on the ground state. The results clarify a two-step dissociation mechanism for methanol and water and show the importance of the ground-state energetics in determining the irreversibility of the dissociation.

EXPERIMENTAL DETAILS

The combination of laser-induced photocatalysis with a mass spectrometer having extremely low background provides a tool to probe photocatalytic chemistry. Figure 1 shows a schematic diagram of the apparatus, which comprises (1) an ultrahigh vacuum system, including a chamber for sample preparation and characterization, a main chamber with a base pressure of 6×10^{-11} Torr where the sample resides for the experiments, an extremely high vacuum quadrupole mass spectrometer for TPD universal detection, and (2) an amplified 1 kHz Ti/sapphire femtosecond laser system with a frequency doubling setup. The sample preparation and characterization chamber is equipped with an Ar^+ ion gun for sample cleaning and a LEED/AES detector for LEED pattern and contamination check. The key element of the apparatus is the extremely low background quadrupole mass spectrometer detector with electron-bombardment ionization. The ionization region is housed in a liquid nitrogen cooled vacuum region that employs a 500 L s^{-1} turbo molecular pump. A liquid nitrogen cooled titanium sublimation pump is also used for this region. Under normal operating conditions, the region with the electron-bombardment ionizer is maintained at 1.5×10^{-12} Torr. This low ambient pressure allows the measurement of temperature-programmed desorption (TPD) signals with very high sensitivity.

The $TiO_2(110)$ surfaces used in the experiments were prepared by repeated cycles of Ar^+ sputtering and UHV annealing at 850 K and were characterized by Auger spectroscopy and LEED to make sure that the surfaces were clean and flat. According to the temperature-programmed desorption (TPD) of water, the $TiO_2(110)$ surface had an oxygen defect density of about 4%.[24]

The photocatalytic methanol dissociation process was studied by irradiating $TiO_2(110)$ surfaces that were dosed with deuterated methanol (CD_3OH) at a surface temperature of 100 K and then conducting TPD measurements of various desorbed species to probe the parent CD_3OH molecules and the reaction products. CD_3OH, with a purity of >99.9%, was purchased from Sigma-Aldrich. Before use, it was purified further by several freeze−pump−thaw cycles. The surface was dosed with a 0.5 ML (1 ML = 5.2×10^{14} molecules cm^{-2}) coverage of CD_3OH using a home-built, calibrated molecular beam doser. The irradiating laser light had a nominal wavelength of 400 nm, a pulse width of ~50 fs and a bandwidth of ~20 nm. The average power of the light was 460 mW. The laser irradiation area on the surface was the elliptical projection of a 6 mm diameter laser beam with an angle of about 30° between the surface parallel and laser direction. The laser flux on the surface was about 1.3×10^{18} photons cm^{-2} s^{-1}. The $TiO_2(110)$ surface was annealed in vacuum at 850 K for 20 min between TPD experiments to flatten and clean the surface.

COMPUTATIONAL METHODS

All calculations were performed with the Vienna ab initio simulation package (VASP)[25,26] and PAW potential.[27] The wave function was expanded by plane wave with kinetic cutoff of 400 eV and density cutoff of 650 eV. The generalized gradient approximation (GGA) with

dx.doi.org/10.1021/ja304049x | J. Am. Chem. Soc. 2012, 134, 13366−13373

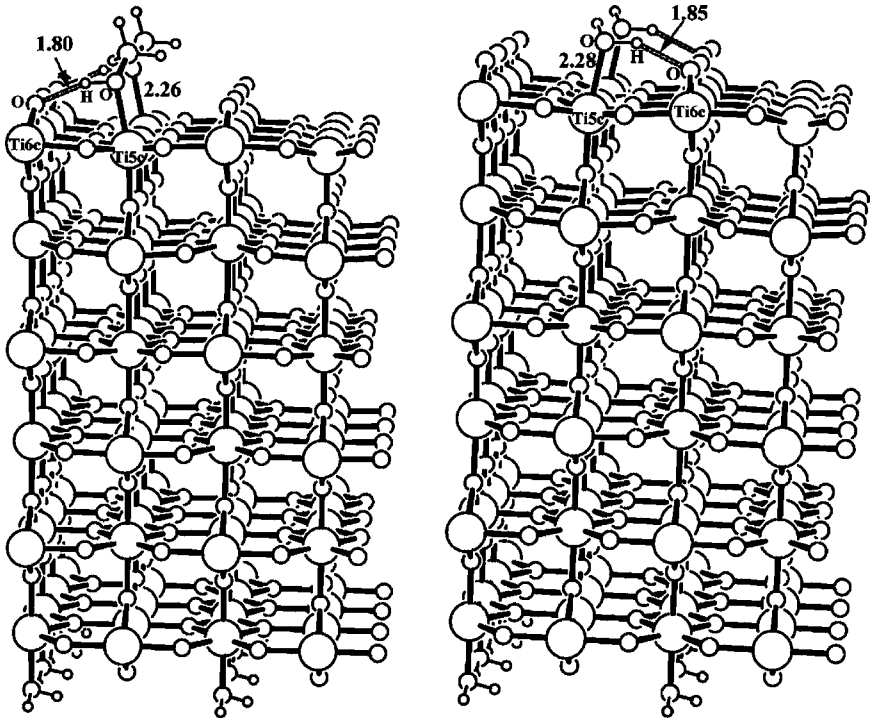

Figure 2. Models used in the calculations. Left: optimized structure for CH_3OH adsorbed on a $TiO_2(110)$ surface. Right: optimized structure for H_2O adsorbed on a $TiO_2(110)$ surface.

the spin-polarized Perdew–Burke–Ernzerhof (PBE) functional[28] was used for all of the calculations. The surface was modeled with a six-layer slab cut out of a TiO_2 crystal to expose the 110 surface. All Ti_{5c} sites on the bottom layer were saturated by water molecules to maintain the coordination environment in bulk. The periodically repeated slabs were decoupled by 12 Å vacuum gaps. A Monkhorst–Pack grid[29] of $2 \times 1 \times 2$ k points was used for the 4×2 surface unit cell. Two molecules were adsorbed on the top layer, and one of them dissociated during the simulation (Figure 2). The chemisorbed species and the top four TiO_2 layers were allowed to relax until the residual forces were less than 0.03 eV/Å, while the remaining atoms were fixed at their bulk truncated positions. Transition states (TSs) were located by constrained minimization and climbing-image nudged elastic band (CI-NEB) methods.[30,31] Isolated gas-phase molecules were optimized in a $(15 \times 15 \times 15)$ unit cell with a single k-point.

The dissociation energy of methanol slightly depends on the methanol concentration on the TiO_2 surface. According to the calculations, in the case of 1/8 ML adsorption the methanol dissociation is slightly exoergic, while for 1/4 ML adsorption or more the methanol dissociation is slightly endoergic. Because in the experiment the actual absorption was significantly larger than 1/8 ML, we used a model with two coadsorbed molecules on the surface to better mimic the experimental condition. In the experiment, only a small fraction of the methanol undergoes dissociation; therefore we treat one molecule as inactive, while the other one dissociates.

As reported previously, the adsorption energies oscillate between odd and even numbers of layers and converge slowly as the number of layers is increased.[32−34] Zhao et al.[35] have studied up to 11-layer-thick slabs, for which the energy differences with respect to the corresponding ten-layer slab are smaller than 0.03 eV. The TiO_2 slab has two sides, where one side is for modeling the surface with the Ti_{5c} sites. The other side is for modeling the bulk, where all Ti atoms are six-coordinated. We use H_2O to saturate the Ti atoms on one side, and these Ti atoms thus have the same coordination number as in the bulk. In test calculations, we found the current model to have less dependence on slab thickness than the model which does not have water saturation. The adsorption and dissociation energy difference between the six-layer slab and the seven-layer slab is smaller than 0.02 eV. The layer convergences of our models were evaluated on a slab with a 2×1 surface unit cell. For six- and seven-layer models, the calculated adsorption energies are 0.71 and 0.72 eV, respectively. The dissociation energies are +0.06 eV and +0.05 eV, respectively. The energy differences between six- and seven-layer models are smaller than 0.02 eV, so the six-layer model is adequate to provide reliable results. The adsorption energy and dissociation energy of CH_3OH were calculated with Monkhorst–Pack grids of $2 \times 1 \times 2$, $3 \times 1 \times 2$, and $2 \times 1 \times 3$ k points. The results are essentially the same, which suggest that the Monkhorst–Pack grid of $2 \times 1 \times 2$ k points is sufficient for the current model. The reported energies are electronic energies without ZPE correction; therefore, they are the same for CH_3OH and CD_3OH, which is used in the experiment.

EXPERIMENTAL RESULTS

Figure 3A shows TPD spectra collected at a mass-to-charge ratio (m/z) of 33 (CD_2OH^+) after surfaces of $TiO_2(110)$ were dosed with CD_3OH and then irradiated by the laser for various durations. The signal profile from $m/z = 33$ is exactly the same as that from $m/z = 35$ (CD_3OH^+, not shown), indicating that the $m/z = 33$ is simply the result of dissociative ionization of the desorbed parent CD_3OH molecule in the electron-bombardment ionizer. The desorbed CD_3OH signal, depicted in Figure 3A, decreases monotonically as the laser irradiation time increases, suggesting that the CD_3OH molecules that are adsorbed on the Ti_{5c} sites of $TiO_2(110)$ are photocatalytically dissociated. The high-temperature side of the CD_3OH TPD peak decreases significantly as the laser irradiation time increases, resulting in a peak shift to lower temperatures. As shown in Figure S1 of Supporting Information (SI), this peak shift is the result of an increased concentration of H or D atoms at BBO sites on the $TiO_2(110)$ surface.

Concomitant to the decrease of the CD_3OH TPD peak, the TPD signal for $m/z = 32$ (CD_2O^+) increases with increasing laser irradiation times (Figure 3B). The CD_2O^+ signal may come from three sources. The formaldehyde (CD_2O) product that is adsorbed molecularly on the surface desorbs with a peak

dx.doi.org/10.1021/ja304049x | J. Am. Chem. Soc. 2012, 134, 13366−13373

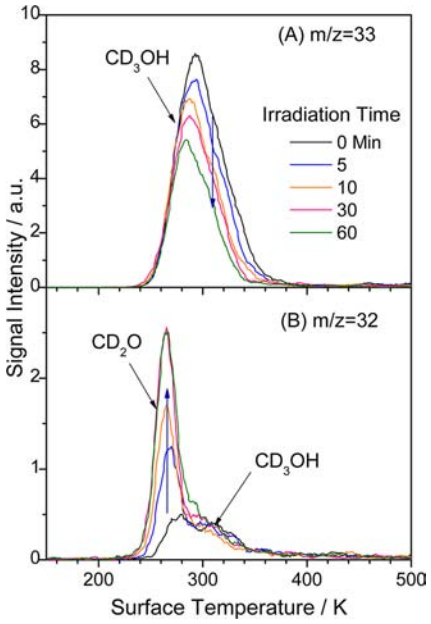

Figure 3. (A) Typical TPD spectra collected at m/z = 33 (CD_2OH^+) following different laser irradiation times. CD_2OH^+ is formed by dissociative ionization of the desorbed parent CD_3OH molecule in the electron-bombardment ionizer. (B) Typical TPD spectra collected at m/z = 32 (CD_2O^+) following different laser irradiation times. The m/z = 32 signal has three components: the parent ion signal of formaldehyde (CD_2O), as well as the ion-fragment signals of the parent CD_3OH molecule and the photocatalyzed CD_3OD product.

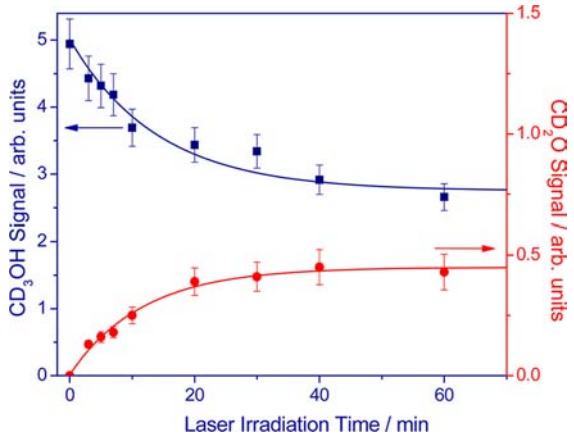

Figure 4. Integrated TPD signals of the desorbed parent methanol (CD_3OH) signal (from m/z = 33) and the formaldehyde (CD_2O) product as a function of laser irradiation time. The CD_2O signals were integrated from the m/z = 32 TPD spectra after the contributions from CD_3OH and CD_3OD had been subtracted. The decrease of the parent methanol signal correlates almost perfectly with the rise of the formaldehyde signal.

in the TPD spectrum near 270 K.[36] The other two sources of CD_2O^+ signal are dissociative ionization of adsorbed parent CD_3OH molecules and CD_3OD reaction products. Both CD_3OH and CD_3OD desorb in the same temperature range, with a broad peak near 300 K, but the presence of both species is confirmed by their detection at their respective parent mass-to-charge ratios of 35 and 36 (see Figure S2, Supporting Information). After a laser irradiation time of 30 min, the CD_3OD signal at m/z = 36 is about 15% of the CD_3OH signal at m/z = 35 (Figure S2, Supporting Information). The CD_3OD products are evidently formed through recombination reactions following dissociation of CD_3OH. In particular, the detection of CD_3OD suggests that CD_3O combines with a D atom.

The large TPD signal for desorbed CD_2O seen in Figure 3B indicates that formaldehyde is an important photocatalytic product. Figure 4 shows that the increase in the formaldehyde signal with laser irradiation time is almost perfectly anticorrelated with the decrease in the signal from the adsorbed parent CD_3OH, strongly suggesting that formaldehyde is the main product of photocatalyzed dissociation of CD_3OH on TiO_2(110). The decrease of the CD_3OH signal with increased irradiation time is not the result of desorption of CD_3OH during laser irradiation, as we observed no CD_3OH signal during irradiation. In fact, a tiny signal from formaldehyde was detected during irradiation (by time-of-flight methods), indicating that photocatalysis can lead to the production of formaldehyde. In order to produce formaldehyde from methanol, the CD_3OH molecule must lose one hydrogen atom and one deuterium atom from the hydroxyl group and the fully deuterated methyl group, respectively.

Thus, the observation of both CD_3OD and CD_2O points to a two-step dissociation of CD_3OH through a CD_3O intermediate. CD_3OH first dissociates to CD_3O on a Ti_{5c} site, where the CD_3OH binds to TiO_2(110), and an H atom. Because the adsorption of H atoms on the surface-bonded oxygen (SBO) sites is energetically much less favorable than adsorption on the BBO sites,[37] the dissociated H atoms from CD_3OH would be expected to adsorb on the BBO sites. Secondary dissociation of a D atom from intermediate CD_3O produces CD_2O on a Ti_{5c} site and a D atom, which also likely binds to a BBO site. This reaction sequence thus explains the formation of CD_2O as well as CD_3OD. It is also consistent with our previous conjecture from a TD-2PPE study[22] that photocatalysis of methanol occurs mostly on the Ti_{5c} sites and not on BBO defect sites.

The stepwise dissociation of CD_3OH and the affinity of H and D for the BBO sites are confirmed by TPD measurements of the water product isotopologues, H_2O, HOD, and D_2O. TPD spectra were collected at m/z = 18 (H_2O^+, CD_3^+), 19 (HOD^+), and 20 (D_2O^+) following laser irradiation of varying duration. Typical TPD spectra for these three m/z ratios are shown in Figure 5. The TPD spectra of these products have maxima near 450 K and the magnitudes of the signals clearly depend on the laser irradiation time. The observed TPD spectra for H_2O, HOD, and D_2O are very similar to the H_2O TPD peak that is known to originate from H atoms adsorbed on the BBO sites of TiO_2(110),[38] suggesting that the TPD signals of all the water isotopologues that we observe also come from BBO sites with adsorbed H and D atoms, which are produced by photocatalyzed dissociation of CD_3OH on Ti_{5c} sites. The TPD signal as a function of laser irradiation time for the different water isotopologues provides a comparison between the rates of producing hydrogen atoms bound to bridge-bonded oxygen atoms (BBO-H) and deuterium atoms bound to bridge-bonded oxygen atoms (BBO-D). Using ionizer fragmentation patterns for the water isotopologues that have been measured in our laboratory, the OD^+ contributions to the signal at m/z = 18 that come from HOD and D_2O were subtracted. The relative TPD signals of H_2O, HOD, and D_2O as a function of laser irradiation were then determined (see Figure 6), assuming that the detection efficiencies for the three isotopologues are the same. The results show that the TPD signals rise monotonically as laser irradiation time increases. The rate of increase in TPD signal intensity with laser

dx.doi.org/10.1021/ja304049x | J. Am. Chem. Soc. 2012, 134, 13366−13373

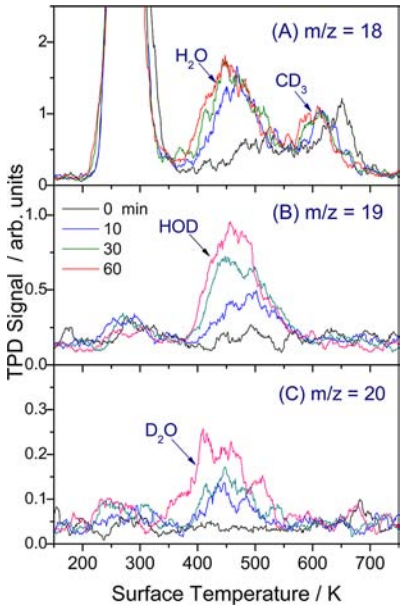

Figure 5. TPD spectra collected at m/z = 18, 19, and 20 from the photocatalysis of $CD_3OH/TiO_2(110)$ with the four different laser irradiation times indicated.

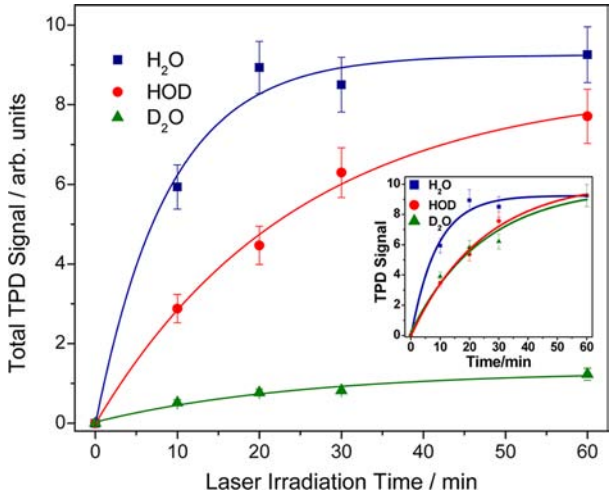

Figure 6. Integrated TPD signals of the water isotopologues as a function of laser irradiation time. The inset shows the same data where the integrated TPD signals of HOD and D_2O have been normalized to the TPD signal of H_2O with 60 min of laser irradiation time.

irradiation time for the HOD and D_2O signals are similar to each other, while the TPD signal intensity for H_2O increases initially with a significantly higher rate (see inset in Figure 6, where the TPD signals of HOD and D_2O are normalized to the TPD signal of H_2O with 60 min of laser irradiation time). The relatively high rate of H_2O formation indicates that H-atom transfer from the hydroxyl group of CD_3OH to the BBO sites occurs faster than D-atom transfer from the D_3-methyl group. Therefore, photocatalyzed H-atom and D-atom dissociation from CD_3OH, the two steps toward the formation of formaldehyde, do not occur simultaneously or concertedly.

We have attempted to observe evidence for photocatalysis of H_2O on $TiO_2(110)$ under the same conditions as those used for the CD_3OH experiments. Figure 7 shows the TPD spectra of H_2O on $TiO_2(110)$ with and without laser irradiation. The H_2O TPD spectra are identical for laser irradiation times of 0, 30, and 60 min, suggesting that water is not photocatalytically active on the $TiO_2(110)$ surface.

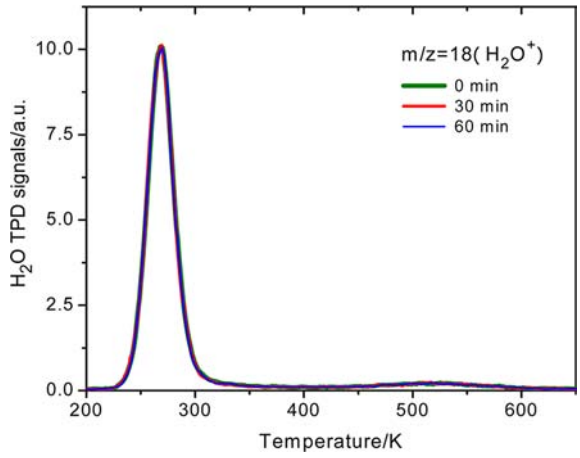

Figure 7. TPD spectra of H_2O on $TiO_2(110)$ with laser surface irradiation (400 nm, 460 mW) for 0, 30, and 60 min.

THEORETICAL RESULTS

The optimized CH_3OH and H_2O adsorbed structures are shown in Figure 2. The average adsorption energy for CH_3OH is calculated to be 0.75 eV. The O−H dissociation energy is slightly endoergic by 0.03 eV, with a barrier of 0.25 eV. The second dissociation step is C−H bond breaking to produce CH_2O and H. This step is highly endoergic (1.03 eV), and the barrier is also much higher (1.57 eV). The barrier for the reverse reaction is therefore 0.54 eV. The optimized transition states and dissociated structures are shown in Figures S3 and S4 (Supporting Information), respectively. After O−H dissociation, the Ti_{5c} site at the reaction position is elevated (by 0.57 Å) and the Ti−O bond becomes shorter. The following C−H dissociation step results in weakly coordinated CH_2O; hence, the elevated Ti_{5c} returns to its original position. The optimized Ti−OCH_2 distance, 2.48 Å, is longer than the 2.26 Å for Ti−$O(H)CH_3$, implying that the adsorption energy of CH_2O is weaker than that for CH_3OH, which is consistent with our experimental observations.

The average adsorption energy of H_2O, 0.69 eV, is slightly smaller than that for CH_3OH. The energetics of the first O−H dissociation step are quite similar to those for CH_3OH, with a dissociation energy and a dissociation barrier of 0.03 and 0.25 eV, respectively. The second O−H dissociation step is endoergic by 0.35 eV, with a barrier of 0.46 eV. The reverse reaction for the second O−H dissociation has a low barrier of only 0.11 eV. The optimized transition states and dissociated structures for H_2O dissociation on TiO_2 are shown in Figures S5 and S6 (Supporting Information), respectively. The geometry changes for the first O−H dissociation step are similar to those for the analogous O−H dissociation step in CH_3OH, featured by the elevation of the Ti_{5c} at the reaction position (by 0.63 Å) and the change of the Ti−O bond length. However, the second dissociation step is different for H_2O and CH_3OH. The second O−H dissociation step for H_2O results in a very strong Ti═O bond, as indicated by the computed bond length, which is only 1.69 Å. As the Ti−O bond becomes stronger, the elevated Ti_{5c} atom does not go back; it elevates even further by 0.86 Å.

To check the reliability of PBE functional, we have calculated the dissociation energy and barrier of CH_3OH with the hybrid

dx.doi.org/10.1021/ja304049x | J. Am. Chem. Soc. 2012, 134, 13366−13373

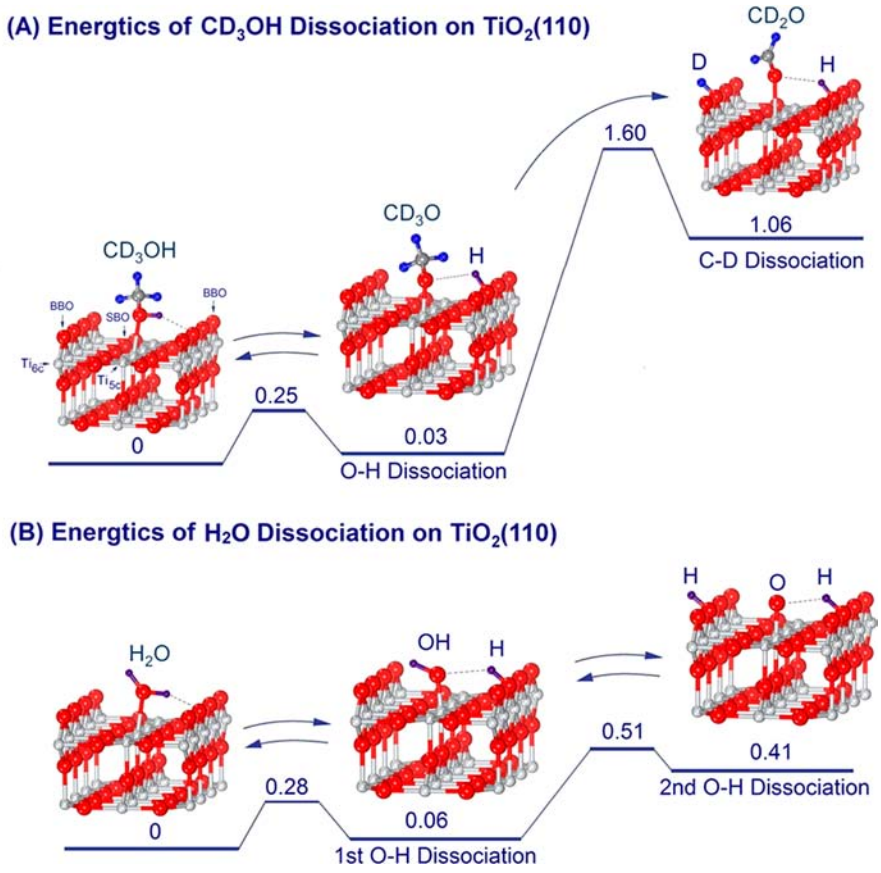

Figure 8. Calculated energetics of the two-step dissociation of (A) CD_3OH and (B) H_2O on the TiO_2(110) surface (see details of theoretical calculations in the Supporting Information). The structures shown are simplified schematics. The exact calculated structures for the adsorption state, dissociated states, and transition states of both methanol and water can be found in Figure 2 and Figures S4−S7, Supporting Information.

functional PBE0,[39] using six-layer slabs made of 2 × 1 unit cells and one CH_3OH molecule adsorbed. The hybrid functional predicts an O−H dissociation energy of 0.07 eV, with a barrier of 0.32 eV. For the same model, the corresponding values for GGA with the PBE functional are 0.06 and 0.20 eV, respectively. These results suggest that GGA with the PBE functional predict reasonable values and trends for the current system. The error for the barrier, about 0.12 eV, does not change the conclusions or the conceptual understanding put forward by this paper.

Oviedo et al.[40] have reported that for a stoichiometric surface, the dissociation of methanol or water on TiO_2 to form a hydroxyl group on in-plane oxygen is much less preferred than on bridge-bonded oxygen. Therefore we only explored the transition states associated with the dissociation to form a hydroxyl group on bridge-bonded oxygen.

■ DISCUSSION

Schematic energy level diagrams for stepwise dissociation of CH_3OH and H_2O are shown in Figure 8. As seen in Figure 8A, our theoretical results show that H-atom dissociation from CD_3OH to a BBO site is nearly thermoneutral with a small barrier (0.25 eV), suggesting that H-atom transfer between methanol and methoxy is facile. This result basically agrees with previous theoretical calculations by Oviedo and co-workers[37,40] and by Sanchez et al.[41] The second step, C−D bond dissociation from CD_3O−Ti_{5c}, is endoergic by 1.03 eV with a barrier of 1.60 eV, likely making it a slower process. The theoretical calculations predict that the lowest energy state for the fully dissociated methanol has formaldehyde bound to a Ti_{5c} site and the hydroxyl and methyl hydrogen atoms having been transferred to two different neighboring BBO rows rather than the same row. Most relevant to photocatalytic dissociation of methanol is the reverse barrier for the D atom to jump back to the adsorbed formaldehyde after any excess energy has been dissipated in the surface. This reverse barrier is quite high, about 0.54 eV, and thus prevents the recombination from occurring efficiently. In addition, the formaldehyde product may desorb from the surface rather than recombine with an H atom because of its weak adsorption on the surface (the adsorption energy of formaldehyde on Ti_{5c} is calculated to be about 0.45 eV). Furthermore, as will be discussed in a future publication, the formaldehyde product may react with methoxy to produce methyl formate, which will desorb from the surface. The desorption and reaction of the formaldehyde product thus make methanol dissociation on the TiO_2(110) surface irreversible.

The experimental results suggest that water is not photocatalytically active on TiO_2(110) at all at 400 nm, in striking contrast to methanol. This observation is consistent with previous observations under real photocatalysis conditions.[13,14] The calculated energetics of H_2O dissociation on TiO_2(110) are shown in Figure 8B. The minimum energy path for the first O−H bond dissociation in H_2O is nearly the same as that for O−H dissociation in methanol, and also in essential agreement with earlier calculations.[40,41] Both processes are easily reversible because of the low barriers. However, the dissociation of the second O−H bond in H_2O has a lower endoergicity and lower

dx.doi.org/10.1021/ja304049x | J. Am. Chem. Soc. 2012, 134, 13366−13373

barrier than those for the analogous C-D dissociation step in methanol. Another important difference is the reverse barrier, which is only 0.11 eV for recombination of O and H but 0.54 eV for recombination of CD_2O and D. The low barrier to recombination of O and H makes this reaction prone to occur even after any excess energy has been dissipated, and the high adsorption energy of O on the Ti_{5c} site (>2 eV)[42] guarantees that the O will remain on the surface long enough to ensure that recombination does occur. In the case of methanol, the high barrier to recombination of CD_2O and D and the weak binding between CD_2O and the Ti_{5c} site make recombination unlikely. The ground-state picture in Figure 8 is not meant to imply that the observed stepwise dissociation of methanol or water necessarily occurs on the ground state. Nevertheless, the ground-state energetics will govern the reverse barriers after two hydrogen atoms have been dissociated, and these reverse barriers explain why methanol photocatalyzes easily on TiO_2(110) while photocatalytic water splitting on this surface is inefficient.

All calculated dissociation barriers and recombination barriers for O−H bonds are low, while for C−H bonds these barriers are much higher. The dissociation reactions involve electrophilic attack of the bridge-bonded oxygen atom by the hydrogen in the O−H/C−H bond. The hydrogen in O−H bond is more electrophilic than in C−H bond (because the electronegativity difference for O/H is larger than that for C/H); therefore, the barrier for O−H dissociation is lower. There is a similar trend for the recombination of H and O or C, which involve electrophilic attack of O/C by hydrogen. Since oxygen bears more negative charge than carbon (because the electronegativity of oxygen is larger), the recombination barrier for O−H dissociation is also lower. In addition, the O−H dissociation does not introduce much geometric rotation, while C−H dissociation results in the rotation of the carbon center from tetrahedral to planar. We have checked the intermediate structures on the reaction path and found that the bond breaking and rotation are simultaneous—there is not an independent barrier for the rotation. This geometrical effect also contributes to a larger barrier for C−H dissociation/recombination than for O−H dissociation/recombination.

Almeida et al.[43] have proposed that the hydration of the surface may influence adsorption/desorption enthalpies of other molecules. Our calculations confirm their result, but the influence is quite small. For example, on our 4 × 2 slab, when one water molecule is adsorbed, the adsorption energy is calculated to be 0.71 eV, while if the slab is preadsorbed by one water molecule, the adsorption energy of a new water molecule is 0.68 eV. The adsorption energies also decrease with the increasing coverage of methanol. The average adsorption energies of methanol for 1/8, 1/4, and 1/2 ML surface coverage are 0.78, 0.75, 0.73 eV, respectively. Therefore, the results reported here should be unaffected by modest surface hydration.

CONCLUSION

In this combined experimental/theoretical study, we have investigated the photocatalytic dissociation of methanol and water on a TiO_2(110) surface. A clear physical picture has emerged for stepwise dissociation of two hydrogen atoms. The high reverse barrier of the second C−H(D) dissociation step of methanol inhibits recombination and is key for efficient methanol dissociation. In the case of water, however, the much lower reverse barrier of the second O−H dissociation step makes recombination facile, thus preventing efficient water splitting. These results suggest that efficient catalysts for water splitting require a high barrier to recombination. In other words, the oxygen atom must be sequestered in a way that will inhibit recombination, just as the oxygen of methanol is sequestered by becoming part of a stable formaldehyde product. The results of the present study clearly show that surface dynamics are very important in understanding photocatalytic chemistry on surfaces.

ASSOCIATED CONTENT

Supporting Information

Effect of BBO-H(D) on the CD_3OH TPD spectra. TPD spectra for CD_3OD versus CD_3OH. Optimized transition states and dissociated structures for stepwise dissociation of CH_3OH and H_2O, from theory. This material is available free of charge via the Internet at http://pubs.acs.org.

AUTHOR INFORMATION

Corresponding Author

fanhj@dicp.ac.cn, tminton@montana.edu, xmyang@dicp.ac.cn

Notes

The authors declare no competing financial interest.

[§]Also with School of Physics and Optoelectric Engineering, Dalian University of Technology, Dalian, Liaoning 59717, China.

[‖]Chinese Academy of Sciences Visiting Senior Scientist.

ACKNOWLEDGMENTS

This work was supported by the Chinese Academy of Sciences, National Science Foundation of China, and the Chinese Ministry of Science and Technology. H.F. acknowledges support from the National Natural Science Foundation of China (No. 21173212). T.K.M. is grateful for support from the Chinese Academy of Sciences Visiting Professorships for Senior International Scientists.

REFERENCES

(1) Henderson, M. A. *Surf. Sci. Rep.* **2011**, *66*, 185−297.
(2) Fujishima, A.; Honda, K. *Nature* **1972**, *238*, 37−38.
(3) Gratzel, M. *Nature* **2001**, *414*, 338−344.
(4) Wahlström, E.; Vestergaard, E. K.; Schaub, R.; Rønnau, A.; Vestergaard, M.; Læsgaard, E.; Stensgaard, I.; Besenbacher, F. *Science* **2004**, *303*, 511−513.
(5) Fox, M. A.; Dulay, M. T. *Chem. Rev.* **1993**, *93*, 341−357.
(6) Linsebigler, A. L.; Lu, G.; Yates, J. T., Jr. *Chem. Rev.* **1995**, *95*, 735−758.
(7) Khan, S. U. M.; Al-Shahry, M.; Ingler, W. B., Jr. *Science* **2002**, *297*, 2243−2245.
(8) Wang, R.; Hashimoto, K; Fujishima, A.; Chikuni, M.; Kojima, E.; Kitamura, A.; Shimohigoshi, M.; Watanabe, T. *Nature* **1997**, *388*, 431−432.
(9) Kamat, P. V. *Chem. Rev.* **1993**, *93*, 267−300.
(10) Zhang, Z.; Bondarchuk, O.; White, J. M.; Kay, B. D.; Dohnalek, Z. *J. Am. Chem. Soc.* **2006**, *128*, 4198−4199.
(11) Chen, X.; Liu, L.; Yu, P. Y.; Mao, S. S. *Science* **2011**, *331*, 746−750.
(12) Hoffmann, M. R.; Martin, S. T.; Choi, W.; Bahnemann, D. W. *Chem. Rev.* **1995**, *95*, 69−96.
(13) Ollis, D. F.; Al-Ekabi, H. *Photocatalytic Purification and Treatment of Water and Air*; Elsevier: Amsterdam, 1993.
(14) Sato, S.; White, J. M. *Chem. Phys. Lett.* **1980**, *72*, 83−86.
(15) Kawai, T.; Sakata, T. *J. Chem. Soc., Chem. Commun.* **1980**, *24*, 694−695.
(16) Diebold, U. *Surf. Sci. Rep.* **2003**, *48*, 53−229.

(17) Bates, S. P.; Gillan, M. J.; Kresse, G. *J. Phys. Chem. B* **1998**, *102*, 2017−2026.
(18) Henderson, M. A.; Otero-Tapia, S.; Castro, M. E. *Faraday Discuss.* **1999**, *114*, 313−329.
(19) Pang, C. L.; Lindsay, R.; Thornton, G. *Chem. Soc. Rev.* **2008**, *37*, 2328−2353.
(20) Onda, K.; Li, B.; Zhao, J.; Petek, H. *Surf. Sci.* **2005**, *593*, 32−37.
(21) Li, B.; Zhao, J.; Onda, K.; Jordan, K. D.; Yang, J.; Petek, H. *Science* **2006**, *311*, 1436−1440.
(22) Zhou, C.; Ren, Z.; Tan, S.; Ma, Z.; Mao, X.; Dai, D.; Fan, H.; Yang, X.; LaRue, J.; Cooper, R.; Wodtke, A. M.; Wang, Z.; Li, Z.; Wang, B.; Yang, J.; Hou, J. *Chem. Sci.* **2010**, *1*, 575−580.
(23) Shen, M; Henderson, M. A. *J. Phys. Chem. Lett.* **2011**, *2*, 2707−2710.
(24) Zehr, R. T.; Henderson, M. A. *Surf. Sci.* **2008**, *602*, 1507−1516.
(25) Kresse, G.; Hafner, J. *Phys. Rev. B* **1993**, *47*, 558−561.
(26) Kresse, G.; Furthmuller, J. *Phys. Rev. B.* **1996**, *54*, 11169−11186.
(27) Blochl, P. E. *Phys. Rev. B* **1994**, *50*, 17953−17979.
(28) Perdew, J. P.; Burke, K.; Ernzerhof, M. *Phys. Rev. Lett.* **1996**, *77*, 3865−3868.
(29) Monkhorst, H. J.; Pack, J. D. *Phys. Rev. B* **1976**, *13*, 5188−5192.
(30) Henkelman, G.; Uberuaga, B. P.; Jonsson, H. *J. Chem. Phys.* **2000**, *113*, 9901−9904.
(31) Henkelman, G.; Jonsson, H. *J. Chem. Phys.* **2000**, *113*, 9978−9985.
(32) Sanchez de Armas, R.; Oviedo, J.; San Miguel, M. A.; Sanz, J. F. *J. Phys. Chem. C* **2007**, *111*, 10023−10028.
(33) Kowalski, P. M.; Meyer, B.; Marx, D. *Phys. Rev. B* **2009**, *79*, 115410.
(34) Stefanovich, E. V.; Truong, T. N. *Chem. Phys. Lett.* **1999**, *299*, 623−629.
(35) Zhao, J.; Yang, J.; Petek, H. *Phys. Rev. B* **2009**, *80*, 235416.
(36) Lu, G.; Linsebigler, A.; Yates, J. T., Jr. *J. Phys. Chem.* **1994**, *98*, 11733−11738.
(37) Sanchez de Armas, R.; Oviedo, J.; San Miguel, M. A.; Sanz, J. F. *J. Phys. Chem. C* **2007**, *111*, 10023−10028.
(38) Yin, X.-L.; Calatayud, M.; Qiu, H.; Wang, Y.; Birkner, A.; Minot, C.; Wöll, Ch. *Chem. Phys. Chem.* **2008**, *9*, 253−256.
(39) Perdew, J.; Ernzerhof, M.; Burke, K. *J. Chem. Phys.* **1996**, *105*, 9982−9985.
(40) Oviedo, J.; Sanchez de Armas, R.; San Miguel, M. A.; Sanz, J. F. *J. Phys. Chem. C* **2008**, *112*, 17737−17740.
(41) Sanchez, V. M.; Cojulun, J. A.; Scherlis, D. A. *J. Phys. Chem. C* **2010**, *114*, 11522−11526.
(42) Tilocca, A.; Selloni, A. *Chem. Phys. Chem.* **2005**, *6*, 1911−1916.
(43) Almeida, A. R.; Moulijn., J. A.; Mul, G. *J. Phys. Chem. C* **2008**, *112*, 1552−156.